Eur. Phys. J. A **27**, 183–186 (2006)
DOI 10.1140/epja/i2005-10265-1

THE EUROPEAN PHYSICAL JOURNAL A

A first experimental approach to the ^{15}O + α elastic scattering

F. Vanderbist[1], P. Leleux[1,a], C. Angulo[1], E. Casarejos[1], M. Couder[1,b], M. Loiselet[1], G. Ryckewaert[1], P. Descouvemont[2], M. Aliotta[3], T. Davinson[3], Z. Liu[3], and P.J. Woods[3]

[1] Institut de Physique Nucléaire et Centre de Recherches du Cyclotron, Université Catholique de Louvain, B-1348 Louvain-la-Neuve, Belgium
[2] PNTPM, Université Libre de Bruxelles, B-1050 Brussels, Belgium
[3] School of Physics and Astronomy, The University of Edinburgh, Edinburgh EH9 3JZ, UK

Received: 8 November 2005 / Revised version: 10 January 2006 /
Published online: 27 March 2006 –
Communicated by J. Äystö

Abstract. The ^{15}O$(\alpha,\alpha)^{15}$O elastic scattering is investigated using a ^{15}O radioactive beam and a He gas cell limited by Mylar windows. The width of a ^{19}Ne state at an excitation energy of 5.35 MeV is measured as $\Gamma_\alpha = 3.2 \pm 1.6$ keV, in agreement with charge symmetry estimate.

PACS. 25.60.-t Reactions induced by unstable nuclei – 27.20.+n $6 \leq A \leq 19$ – 26.30.+k Nucleosynthesis in novae, supernovae, and other explosive environments

1 Introduction

The ^{15}O$(\alpha,\gamma)^{19}$Ne is of interest in explosive burning occurring in X-ray bursts, as this reaction could be a breakout from the hot CNO cycles to the rp-process. The ^{15}O + α threshold is situated at 3.529 MeV in ^{19}Ne, and the ^{15}O$(\alpha,\gamma)^{19}$Ne reaction proceeds through resonances above and close to the threshold; the strength of these resonances is governed by their α width (Γ_α), as the total width is quite close to the γ width. Recent experiments [1–3] have determined Γ_α (or put limits to Γ_α) for levels in ^{19}Ne up to 5.092 MeV excitation energy. A conclusion is that a direct measurement of the ^{15}O$(\alpha,\gamma)^{19}$Ne reaction in the region of astrophysical interest is currently impossible: ^{15}O beams of intensity larger than 10^{11} pps on target would be required indeed to measure the ^{15}O$(\alpha,\gamma)^{19}$Ne cross-section in inverse kinematics in the energy region surrounding the first state above threshold, at 4.033 MeV, for which $\Gamma_\alpha \leq 0.011$ meV [1]. This high beam current is one of the main challenges to be tackled in the coming years.

^{15}O beams of lower intensity have been however developed [4], and they can be used to investigate levels at higher excitation energies. The present work goes along this line: the Γ_α of a state at 1.82 MeV above threshold was measured by the elastic resonant method in inverse kinematics. This state, at an excitation energy of 5.351 MeV in ^{19}Ne, with $J^\pi = 1/2^+$ [5], was observed in the ^{20}Ne$(^3$He$,\alpha)^{19}$Ne reaction [6,7]. It is supposed to be the analog of the 5.337 MeV state in ^{19}F; a recent measurement of the ^{15}N$(\alpha,\gamma)^{19}$F reaction [8] yielded a total width $\Gamma \sim \Gamma_\alpha = 1.3 \pm 0.5$ keV for the latter. Assuming the equality of the reduced widths for analog states and correcting for the different penetrabilities in both cases, $\Gamma_\alpha = 5.4 \pm 2.1$ keV is deduced for the 5.351 MeV level in ^{19}Ne. A few years ago, de Oliveira *et al.* [9] have shown that this procedure was not valid in ^{19}Ne levels between 4.3 and 5.1 MeV excitation energy, the resulting α widths being uncertain by at least a factor of 10. However, in the energy region close to threshold covered in [9], the γ widths are much larger than the α widths. If charge symmetry is expected to be valid for reduced α widths, it is not applicable to the (dominant) $E2$ and $M1$ multipolarities. Accordingly, the conclusions drawn by de Oliveira *et al.* on the α widths, based on the approximation Γ_γ (^{19}Ne) $\simeq \Gamma_\gamma$ (^{19}F) are to be checked. This was done in the present work through the direct measurement of Γ_α for the 5.351 MeV level in ^{19}Ne. In addition, as we will see, using a He gas target will lead to some experimental problems that will require new data analysis methods.

This paper is organized as follows: in sect. 2, the experimental method is described. The ^{15}O + α data analysis is presented in sect. 3 and the results are discussed in sect. 4.

2 Experimental method

2.1 The ^{15}O radioactive beam

The beam was produced by the ISOL method at the RIB facility at Louvain-la-Neuve. A 29.5 MeV proton beam of

[a] e-mail: leleux@fynu.ucl.ac.be
[b] *Present address:* University of Notre Dame, USA.

a 200 μA intensity was accelerated by the CYCLONE30 cyclotron and was stopped in a lithium fluoride target. ^{15}O atoms obtained from the ^{19}F(p, αn)^{15}O reaction were injected in an ECR source, where they were ionized to the 2+ state, and then accelerated in the CYCLONE110 cyclotron, up to an energy of 12.5 MeV. This cyclotron was used also as a mass analyzer. The relative mass difference between ^{15}O and its isobaric stable isotope ^{15}N is about 2 10^{-4}, large enough to allow for a negligible contamination of the ^{15}O beam ($\leq 1\%$) [4]. The ^{15}O beam with an intensity of about 3×10^6 pps was focused on the He target described below.

2.2 The He target

The He gas target should be thick enough to cover in one step the expected resonance width, through the energy loss of the ^{15}O beam in the gas. A 15 mm thick gas cell with a 100 mbar He pressure was used. Along the beam direction, Mylar windows of 2.5 μm thickness and of diameter 12 mm (front) and 30 mm (back) were placed; the beam energy loss in the He gas was about 300 keV [10].

2.3 Detectors

A silicon multistrip annular detector of 300 μm thickness of the LEDA type, *i.e.* 8 sectors of 16 strips each, [11] was located at forward angle, at 23.1 cm from the gas cell center, and covered the laboratory angular domain $\theta_{\rm lab} = 12°$–$29°$ or the center-of-mass range $\theta_{\rm cm} = 122°$–$156°$. Each strip was equipped with associated electronics (ADC and TDC) providing with the measurement of the energy and time-of-flight for each registered event. Figure 1 is a two-dimensional spectrum (time of flight *vs.* energy for a particular strip of LEDA). The time of flight was measured with respect to the cyclotron radiofrequency. Several well-defined regions were easily located, corresponding to: scattered ^{15}O on the windows of the gas target, recoil α-particles from the He gas and recoil protons from the Mylar windows. α-particles in region a) of fig. 1 are clearly separated from other particles.

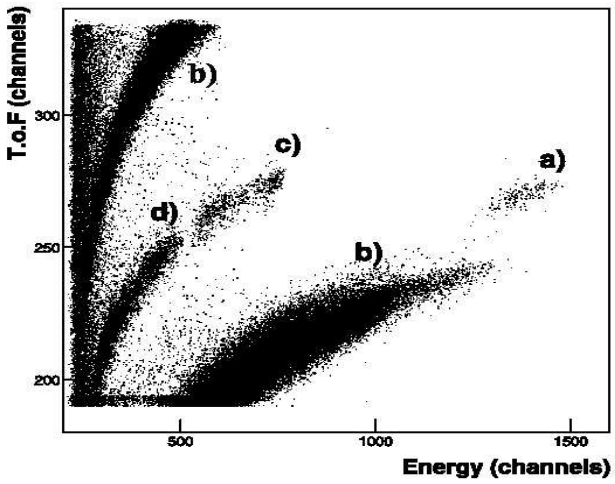

Fig. 1. Two-dimensional spectrum (time of flight *vs.* energy) of particles resulting from the interaction of an ^{15}O beam with a He gas contained within Mylar windows. The marked regions correspond to a) recoil α-particles, b) recoil heavy ions and c), d) recoil protons from the front and the back windows, respectively.

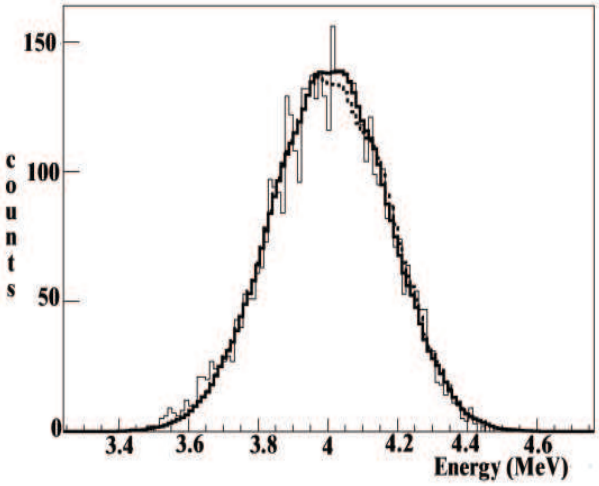

Fig. 2. Typical recoil α-spectrum, obtained at $\theta_{\rm lab} = 16.3 \pm 0.6°$ (histogram). The dotted curve is the best fit without resonance; the solid curve is the best fit with a resonant state.

3 Data analysis

Contrary to the "typical" case of recoil proton spectra from a CH_2 target and a broad resonant state (see, *e.g.*, fig. 1 of [12]), the present α-spectra are featureless, for several reasons: the ^{15}O beam energy loss in the entrance Mylar foil is large ($\sim$ 3.6 MeV), inducing a large straggling; the beam energy loss in the He gas is small ($\sim$ 300 keV); the α-particles energy loss in the exit window is large ($\sim$ 320 keV), as well as their straggling and finally, the opening angle of each LEDA strip is broadened by the longitudinal extension of the gas cell. As a consequence, α-particle spectra at a given angle, obtained as the summation of eight strips, show no obvious pattern revealing the presence of a resonant state (fig. 2). Sixteen of such spectra were obtained. A new method of analysis consisting in a Monte Carlo simulation of the experimental spectra was thus performed. In a first step, events were generated from the gas volume and tracked to the detectors, with a weight equal to the Coulomb cross-section at the corresponding energy and angle. Many quantities are needed to characterize an event: the ^{15}O beam energy and energy width, the beam spot on target, the beam energy loss and straggling in the entrance Mylar window, the entrance and exit

windows thickness, the ^{15}O energy loss and straggling in the He gas, the α-particles energy loss and straggling in the He gas and in the exit Mylar window and, finally, the energy loss of α-particles in the dead layer of the detector. Some of these quantities were fixed, while others were allowed to vary within reasonable limits in order to reproduce the experimental spectra. In the first category came quantities very precisely measured before, or having a negligible impact on the α-spectra, or being strongly linked to another quantity: the ^{15}O energy loss in Mylar, the helium gas thickness and the α-particles energy loss in the detector's dead layer are such examples. The other quantities were allowed to vary within limits quoted in parentheses: the ^{15}O beam energy (± 100 keV), the FWHM of the beam energy distribution (125–250 keV), the beam spot on target (< 1 cm), the beam straggling in Mylar (< 180 keV), the beam energy loss in He ($\pm 20\%$ with respect to SRIM 2003 [10] allowing for the bulging of the windows), the window's thickness ($\pm 2.5\%$), the α-particles energy loss in Mylar ($\pm 10\%$ with respect to SRIM 2003), the α-particles straggling in Mylar (3–5%). A total of nine parameters were thus incorporated in the fit, a typical best fit for a particular angle being shown as the dotted curve in fig. 2.

In a second step, the resonant state was introduced: a simulation containing a resonant state in the R-matrix formalism, in the one-channel one-level approximation [13], was performed. The scattering amplitude is the sum of a Coulomb term and a nuclear term. The latter contains the Coulomb phase shift ω_ℓ and the collision matrix U_ℓ, which is proportional to the factor $\exp 2i\delta^\ell$. The phase shift δ^ℓ is defined by:

$$\delta^\ell = \delta^\ell_{\rm HS} + \delta^\ell_R, \tag{1}$$

where $\delta^\ell_{\rm HS}$ and δ^ℓ_R are the hard-sphere and the R-matrix phase shifts, respectively. Here, we have used R-matrix phase shifts for $\ell = 0$, all other partial waves being treated with the hard-sphere formalism (we have checked that ℓ-values larger than 1 are negligible). Thus

$$\delta^0_R = \arctan \frac{P_0 R^0}{1 - S_0 R^0}, \tag{2}$$

where P_0 and S_0 are the $\ell = 0$ penetration and shift factors, respectively, and R^0 is the R-matrix defined with a single pole. In general, the fitted parameters are the pole parameters converted [14] to the resonance energy $E_{\rm R}$ and the alpha width Γ_α of the state in ^{19}Ne (in R-matrix notation, E_α and Γ_α are "observed" parameters). Here, the resonance energy was kept equal to 1.82 MeV, the only parameter of the fit being Γ_α of the state. The other quantities of the simulation kept their values obtained at the end of step 1. In fig. 2, the solid curve is the result of the best fit with Γ_α as a parameter. A difference between both curves is observed in the central part of the spectrum, in the region where the resonance is expected to play a role: the upper and lower slopes are indeed governed by the energy loss and straggling of ^{15}O beam ions and outgoing α-particles. Figure 3 shows the normalized χ^2 *vs.* Γ_α. The introduction of this new (tenth) parameter improved the χ^2 by 25%. From the $(\chi^2_{\rm min} + 1)$ procedure, $\Gamma_\alpha = 3.2 \pm 1.6$ keV was deduced.

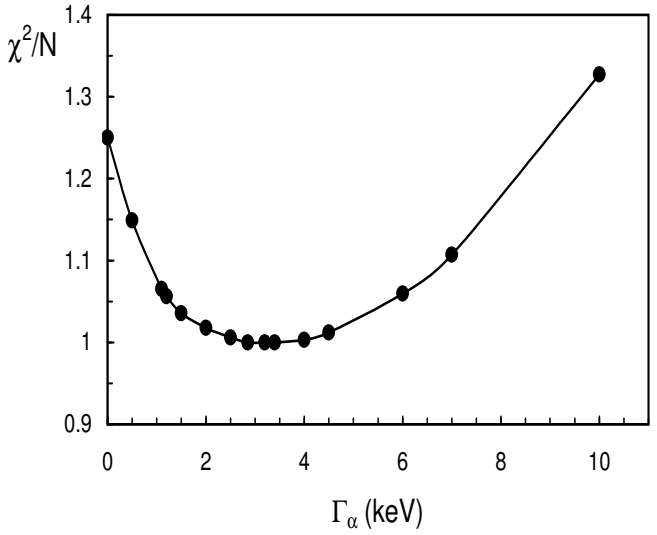

Fig. 3. Normalized χ^2 (*i.e.* χ^2 divided by the number of degrees of freedom) *vs.* Γ_α (keV), resulting from the global fit of the α-spectra from the $^{15}O(\alpha,\alpha)$ elastic scattering. The solid curve is an eye guide.

In order to gain confidence in the significance of this width determination, a second analysis of the experimental spectra was performed. In each spectrum, the content of each energy bin was modified according to the Poisson law and a global fit of the new spectra was done as in the second step of the previous analysis, with the α width as parameter; a width (Γ_i) corresponding to the minimum χ^2 was then obtained. This process was repeated up to 15 times, a mean width $\Gamma_{\rm m}$ was deduced as the average of the fifteen Γ_i's and the error (σ) was calculated by external consistency:

$$\sigma = \sqrt{\frac{\Sigma_i(\Gamma_{\rm m} - \Gamma_i)^2}{15 \times 14}}$$

The result of this second analysis, $\Gamma_{\rm m} = 2.9 \pm 1.8$ keV, in perfect agreement with the first one makes us confident that the improvement of the χ^2 in the second step of the first analysis was not due to a statistical effect.

4 Discussion

A first measurement of the width of a resonant state in ^{19}Ne was performed through the $^{15}O(\alpha,\alpha)$ elastic scattering in inverse kinematics, using an ^{15}O radioactive beam and a He gas cell. The trend of χ^2 *vs.* Γ_α (fig. 3) clearly shows that the width of the resonant state is around 3 keV, unfortunately with a large uncertainty due to the flat shape of χ^2. The deduced width of the 5.351 MeV level in ^{19}Ne, *i.e.* 3.2 ± 1.6 keV, is in agreement with the width obtained from its analog state at 5.337 MeV in ^{19}F, *i.e.* 5.4 ± 2.1 keV, confirming the validity of charge symmetry for α widths. However, large error bars (both in the ^{19}F

and the ^{19}Ne levels) preclude a precision check of the extrapolation procedure of α widths between analog states in light nuclei.

The limitations of the present set-up were noticed, compared to previous experiments performed in the same lab in which recoil protons were detected from a solid CH_2 target [15]: the longitudinal extension of the gas target and the degradation of the beam due to Mylar windows were the most important factors affecting the quality of the α-recoil spectra. As an attempt to bypass both problems, thin Al foils were recently implanted with He ions. For 50 μg/cm^2 thick Al foils, encouraging results were obtained regarding the homogeneity of the implantation *vs.* the foil thickness and regarding the total amount of He implanted [16]. For most resonant states, thicker foils are, however, required.

We thank the staff of the Cyclotron Research Center, Louvain-la-Neuve, for the production of the ^{15}O beam and the technical support during the experiment. This work has been supported by the Interuniversity Attraction Poles Programme of the Belgian Science Policy (P5/07) and by the UK Engineering & Physical Science Research Council (EPSRC). P.D. and P.L. are Research Director of the National Fund for Scientific Research (FNRS), Belgium.

References

1. B. Davids *et al.*, Phys. Rev. C **67**, 012801(R) (2003).
2. D.W. Visser *et al.*, Phys. Rev. C **69**, 048801 (2004).
3. P.V. Magnus *et al.*, Nucl. Phys. A **506**, 332 (1990).
4. M. Gaelens *et al.*, *Proceedings of the Fifteenth International Conference on Applications of Accelerators in Research and Industry, Denton, 1998*, edited by J.L. Duggan, I.L. Morgan, AIP Conf. Proc. **475**, 305 (1999).
5. D.R. Tilley *et al.*, Nucl. Phys. A **595**, 1 (1995).
6. J. Garrett *et al.*, Phys. Rev. C **2**, 1243 (1970).
7. D.S. Haynes *et al.*, Phys. Rev. C **5**, 5 (1972).
8. S. Wilmes *et al.*, Phys. Rev. C **66**, 065802 (2002).
9. F. de Oliveira *et al.*, Phys. Rev. C **55**, 3149 (1997).
10. J.F. Ziegler, J.P. Biersack, U. Littmark, *The Stopping and Range of Ions in Solids* (Pergamon, New York, 1985); J.F. Ziegler, J.P. Biersack, SRIM programme V2003.26.
11. T. Davinson *et al.*, Nucl. Instrum. Methods A **454**, 350 (2000).
12. R. Coszach *et al.*, Phys. Rev. C **50**, 1695 (1994).
13. A.M. Lane, R.G. Thomas, Rev. Mod. Phys. **30**, 257 (1958).
14. C. Angulo, P. Descouvemont, Phys. Rev. C **61**, 064611 (2000).
15. Th. Delbar *et al.*, Nucl. Phys. A **542**, 263 (1992); C. Angulo *et al.*, Nucl. Phys. A **716**, 211 (2003); C. Angulo *et al.*, Phys. Rev. C **67**, 014308 (2003).
16. F. Vanderbist *et al.*, Nucl. Instrum. Methods B **197**, 165 (2002).